Missile and Spacecraft Coning Instabilities

D. H. Platus*
The Aerospace Corporation, El Segundo, California 90245

The destabilizing effect of yaw or Magnus-type moments on the angle-of-attack behavior of spinning missiles is well known to the missile designer. Yaw moments can also have a destabilizing (or stabilizing) effect on the attitude or coning motion of spinning spacecraft. The analogy might not be readily apparent because of the difference between the angle of attack of a spinning missile in atmospheric flight and the coning angle of spin-stabilized spacecraft. A concise treatment of the dynamics associated with coning instabilities is presented, and illustrative examples of classical missile and spacecraft coning instabilities are reviewed.

Nomenclature

C_{L_α}	= lift force derivative
$C_{L_\alpha}^*$	= $C_{L_\alpha} q_\infty S / m u$
C_{ℓ_p}	= roll damping coefficient
$C_{\ell_p}^*$	= $C_{\ell_p} q_\infty S d^2 / 2u$
C_{m_q}	= pitch damping derivative
$C_{m_q}^*$	= $-C_{m_q} q_\infty S d^2 / 2 I u$
$C_{m_{\dot\alpha}}$	= damping moment derivative
$C_{m_{\dot\alpha}}^*$	= $C_{m_{\dot\alpha}} q_\infty S d^2 / 2 I u$
$C_{n_{p\alpha}}$	= Magnus moment derivative
$C_{n_{p\alpha}}^*$	= $C_{n_{p\alpha}} q_\infty S d^2 / 2 I u$
d	= aerodynamic reference diameter
F	= vector force
g	= acceleration due to gravity
h	= angular moment vector
I	= pitch or yaw moment of inertia
I_x	= roll moment of inertia
k	= pitch or yaw radius of gyration
L	= lift force
L_θ	= lift force derivative
ℓ	= jet-damping moment arm; $I/m x_s$
M	= vehicle mass
M	= vector moment
$\dot M$	= vehicle mass rate of change; propellant mass flow rate
m	= damper mass; missile mass
p	= roll rate
p_{crit}	= critical roll rate
p_r	= $\mu p / 2$
q	= pitch rate
q_∞	= dynamic pressure
r	= yaw rate; slag mass radial position; missile c.g. coning radius
S	= aerodynamic reference area
T	= rocket thrust
t	= time
u	= missile forward velocity
V	= velocity vector
v	= missile lateral velocity due to coning
X, Y, Z	= nonrotating coordinates
x, y, z	= body-fixed coordinates
x_s	= static margin
y	= center-of-mass offset
$\tilde\alpha$	= angle of attack
$\tilde\beta$	= angle of sideslip
ζ	= damping ratio

Θ	= total angle of attack
Θ_T	= zero roll rate trim angle of attack
θ	= coning angle (Euler angle)
$\dot\theta$	= coning angle rate of change
λ	= precession damping exponent; p/p_{crit}
$\lambda_{1,2}$	= precession damping exponent
μ	= I_x / I
ν	= damping parameter
ν_m	= yaw moment parameter
ξ, η, ζ	= precessing coordinates
$\tilde\xi$	= complex angle of attack, $\tilde\beta + i\tilde\alpha$
τ	= trim force
ϕ	= spin angle relative to θ plane (Euler angle)
$\dot\phi$	= spin rate relative to θ plane
ψ	= precession angle (Euler angle)
$\dot\psi$	= precession rate
$\dot\psi_{1,2}$	= precession rates
$\dot\psi_{+,-}$	= precession rates
Ω	= $(p_r^2 + \omega^2)^{1/2}$
ω	= natural pitch frequency
ω	= angular velocity vector

Introduction

ANYONE who has worked to some degree with the gyroscopic motion of spinning missiles or spacecraft has undoubtedly discovered that the Achilles heel of the vehicle with regard to angle of attack or attitude stability is the "yaw" moment or "side" moment or "Magnus-type" moment, all of which refer to a similar type of disturbance. Because the general epicyclic angle-of-attack motion of a spinning missile is a superposition of two coning motions, one could argue, with few exceptions, that all missile dynamic instabilities are coning instabilities caused by a yaw moment disturbance that effectively undamps one coning motion while damping the other.[1-4] Nicolaides, in an early paper on the flight dynamics of modern ballistic missiles,[5] commented that "all flight dynamic instabilities observed by the writer have been observed to be ultimately of the pure circular type." Referring to "catastrophic yaw" in the same paper, he remarked that the pitching and yawing motion "begins to grow and may very soon reach extreme values such that the missile in flight looks more like a propeller than an arrow."

Similarly, spin-stabilized spacecraft have exhibited coning instabilities in which the angle between the spin axis and the space fixed angular momentum vector grows to excessive values. It is shown that this occurs from energy dissipation when the spin axis is one of minimum moment of inertia.[6] This coning motion can be damped by an actively driven unbalanced rotor or pendulum mass that is quite small relative to the mass of the spacecraft.[7] A similar passive damper consists of a small mass of viscous fluid contained in an annulus that rotates at the precession frequency and damps the coning angle when the spin axis is that of maximum moment of inertia.[8]

In both cases, the action of the small mass imbalance produces a small, stabilizing yaw moment. The passively damped pendulum or

annular fluid damper produces a positive, destabilizing yaw moment if the spin axis is that of minimum moment of inertia. A destabilizing yaw moment is also produced by an oscillating liquid in a spinning shell. This was first demonstrated by Stewartson for an inviscid liquid in a spinning top.[9] Yaw moment effects similar to fluid sloshing can also be produced by internal moving parts in spinning projectiles.[10-12]

Recent launches of a class of spin stabilized vehicles consisting of a spacecraft and a payload assist module (PAM) upper stage have exhibited a coning instability during the latter part of the rocket motor burn.[13-17] This has attracted much attention in the engineering community because virtually all of the launches consisting of a payload attached to a PAM solid rocket motor have exhibited this coning growth, whereas no other comparable vehicle (with perhaps one exception[13]) has shown such behavior. Various attempts have been made to explain the source of the observed coning in terms of a compliant nozzle, nozzle entrance flow asymmetry, spinning body flowfield effects, and slag sloshing effects. There is no satisfactory explanation to date of the actual cause of the coning instability, although a study of the oscillatory motion of a small spring-restrained mass to simulate slag sloshing in the presence of thrust[15] showed that an instability could occur. The analysis led to the not surprising conclusion that the oscillation frequency and phase must be such to produce a yaw moment.

Because of the striking similarity of the forcing function required to cause coning instabilities in spinning bodies, whether they are spin-stabilized spacecraft in a near-moment-free environment or high-speed missiles subject to large aerodynamic forces and moments, it is instructive to derive the general conditions required for spinning-body coning instabilities and apply them to familiar missile and spacecraft coning phenomena. It is convenient for this analysis to use the classical Euler angle coordinates because of the simplicity afforded by the conditions of quasisteady coning motion and the simple geometrical interpretation of the disturbance forces and moments required.

Equations of Motion

The rigid-body motion of a nominally axisymmetric missile or spacecraft is described by the general force and moment equations

$$\frac{F}{m} = [\dot{V}] + \omega \times V \tag{1}$$

$$M = [\dot{h}] + \omega \times h \tag{2}$$

where ω is the angular velocity of a rotating coordinate frame in space, V is the velocity of the center of mass relative to the rotating coordinates, h is the angular momentum of the body with respect to the rotating coordinates, and F and M are the forces and moments acting on the body along and about the coordinate axes, respectively. The classical Euler angle coordinates are shown in Fig. 1, in which X, Y, and Z are nonrotating, space-fixed axes, and ξ, η, and ζ are the rotating coordinate axes from which we derive the equations of motion. We consider the axis of symmetry of our nominally axisymmetric body to lie initially along the space-fixed X axis. The axes ξ, η, and ζ are obtained from X, Y, and Z by a rotation (or precession) ψ about X followed by a rotation θ (or pitch) about η. The angular velocity ω of our rotating frame ξ, η, ζ in space with respect to the ξ, η, ζ axes is

$$\omega = (\dot{\psi}\cos\theta, \dot{\theta}, \dot{\psi}\sin\theta) \tag{3}$$

or, for small θ,

$$\omega \approx (\dot{\psi}, \dot{\theta}, \dot{\psi}\theta) \tag{4}$$

If we consider the further rotation ϕ about the coordinate axis ξ, then the axes x, y, z are conventional body-fixed axes commonly used to describe aircraft or missile motion. Note that the body-fixed axes y and z rotate about ξ with the spin rate $\dot{\phi}$ with respect to the $\xi\zeta$ plane such that the resultant body angular rate p in space about ξ or x is the coordinate angular rate $\dot{\psi}\cos\theta$ plus the spin rate $\dot{\phi}$, or, for small θ,

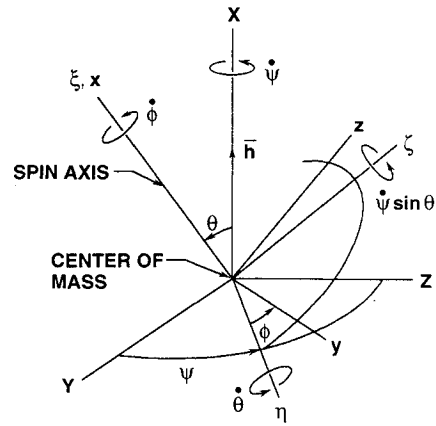$$p \approx \dot{\psi} + \dot{\phi} \tag{5}$$

Fig. 1 Classical Euler angle coordinate system.

The corresponding pitch and yaw rates about the body-fixed axes y and z, from Fig. 1, are

$$q = \dot{\theta}\cos\phi + \dot{\psi}\theta\sin\phi \tag{6}$$

$$r = \dot{\psi}\theta\cos\phi - \dot{\theta}\sin\phi \tag{7}$$

The angular momentum vector h with respect to the rotating coordinates ξ, η, ζ is, for small θ,

$$h = (I_x p, I\dot{\theta}, I\dot{\psi}\theta) \tag{8}$$

where I_x, I, and I are mass moments of inertia about the axes ξ, η, ζ (or x, y, z), respectively, for the axisymmetric body.

The moment equations of motion for a constant mass body in the Euler angle coordinates are obtained by substituting Eqs. (4) and (8) into Eq. (2), which gives

$$\frac{M_\xi}{I_x} = \dot{p} \tag{9}$$

$$\frac{M_\eta}{I} = \ddot{\theta} + (\mu p - \dot{\psi}\theta)\dot{\psi}\theta \tag{10}$$

$$\frac{M_\zeta}{I} = \frac{d}{dt}(\dot{\psi}\theta) + (\dot{\psi} - \mu p)\dot{\theta} \tag{11}$$

where $\mu \equiv I_x/I$.

Yaw Moment Damping or Undamping

Consider, first, the moment-free body in steady coning motion, $\theta = $ const. It follows from Eqs. (9–11) and Eq. (5) that

$$p = \text{const} \tag{12}$$

$$\dot{\psi} = \mu p \tag{13}$$

$$\dot{\phi} = p(1 - \mu) \tag{14}$$

The body precesses about X at the rate μp with the coning angle θ and spins with respect to the $\xi\zeta$ plane with the rate $p(1 - \mu)$. Note that for $\mu < 1$ the spin rate $\dot{\phi}$ is in the same direction as the coning rate $\dot{\psi}$ and for $\mu > 1$ it is in the opposite direction. Yaw moment undamping is the growth in the coning angle θ caused by a positive net yaw moment M_ζ in Eq. (11). A negative yaw moment will cause a decay in θ. The response of the coning angle to an applied yaw moment M_ζ, compared with the response to a pitch moment M_η, is seen most readily if we apply both pitch and yaw moments of the form

$$\frac{M_\eta}{I} = \sigma\kappa\theta \tag{15}$$

$$\frac{M_\zeta}{I} = \kappa\theta \tag{16}$$

where σ is a multiple that determines the size of the pitch moment relative to the yaw moment. If we substitute Eqs. (15) and (16) into

Eqs. (10) and (11), we find for the quasisteady conditions $\ddot{\theta} \approx 0$ and $\dot{\psi} \approx$ const that the motion is composed of two coning motions with coning rates

$$\dot{\psi}_{1,2} = \mu p - \frac{\sigma\kappa}{\mu p}, \qquad \frac{\sigma\kappa}{\mu p} \tag{17}$$

and amplitudes, from Eq. (11), described by

$$\dot{\theta} - \lambda_{1,2}\theta = 0 \tag{18}$$

where

$$\lambda_{1,2} = \frac{\kappa}{2\dot{\psi} - \mu p} = \pm\kappa\left(\mu p - \frac{2\sigma\kappa}{\mu p}\right)^{-1} \tag{19}$$

On integrating Eq. (18), we see that the two motions grow and decay according to

$$\theta = \theta_0 \exp(\lambda_{1,2}t) \tag{20}$$

For a pure yaw moment, $\sigma = 0$, the coning rate is unchanged from Eq. (13), and the coning angle grows exponentially according to

$$\theta = \theta_0 \exp\left(\frac{\kappa}{\mu p}t\right) \tag{21}$$

Consider a spin-stabilized spacecraft with $\mu p = \pi$ rad/s and let $\kappa = 0.02$. For combined pitch and yaw moments with $\sigma = 10$ such that the pitch moment is 10 times the magnitude of the yaw moment, the effect of the pitch moment is to reduce the fast coning frequency, from Eq. (17), by only about 2% and to increase the magnitude of the exponent $\lambda_{1,2}$ by about 4%. The fast mode $\dot{\psi}_1 = 0.98\ \pi$ rad/s grows exponentially with a time constant $\tau = 1/\lambda_1$ of 151 s, and the slow mode $\dot{\psi}_2 = 0.2/\pi$ rad/s decays with the same time constant.

Spacecraft Precession Damper

A damper that has been used to damp the coning motion of a spin-stabilized spacecraft is readily described in terms of yaw moment damping. Consider a precessing spacecraft that contains a small pendulum mass free to rotate about the spacecraft axis of symmetry in a plane a distance h from the spacecraft center of mass, as shown in Fig. 2. The mass could be a slug of liquid contained in an annular cavity, which is a type of device actually flown to damp spacecraft coning motion.[18-23] If the mass or slug of fluid is free of any drag or viscous damping forces, it will assume a steady-state orientation at $\phi_d = 0$ in the negative ζ direction due to centrifugal force from the steady precession $\dot{\psi}$. Because the spacecraft spins at the rate $\dot{\phi}$ relative to the $\xi\zeta$ or θ plane, the mass rotates at the rate $\dot{\phi}$ relative to the spacecraft. Any viscous damping or drag on the mass will displace it at some positive or negative angle ϕ_d from the θ plane, depending on the direction of $\dot{\phi}$, giving rise to a yaw moment. The yaw moment is simply the component of centrifugal force $m\dot{\psi}^2 R$ acting in the η direction times its moment arm h, or

$$M_\zeta = m\dot{\psi}^2 Rh\sin\Phi \tag{22}$$

where the magnitude of R is a function of the coning angle θ. For $\mu < 1$, the spin rate $\dot{\phi}$, from Eq. (14), is positive, which would produce positive Φ as shown in Fig. 2 and a positive yaw moment. In such a vehicle, a passive damped rotor or viscous fluid annular damper would undamp the coning motion. Note also that any viscous or drag force that rotates the pendulum out of the θ plane produces an opposite roll torque that will change the roll rate accordingly. For the slender spacecraft, $I_x < I$, yaw moment undamping of the coning motion is accompanied by a decrease in the roll rate. For spacecraft configurations with $\mu > 1$, for which the passive precession damper was devised, the spin rate $\dot{\phi}$ is negative for positive $\dot{\psi}$, and the mass will be driven in the opposite direction such to produce a negative Φ and negative yaw moment. Because the pendulum rotates relative to the spacecraft in the same direction as $\dot{\psi}$, in this case, it will exert a positive roll torque on the spacecraft via the viscous or drag forces and increase its roll rate. Precession damping can be accomplished in the slender spacecraft, $\mu < 1$, by actively driving an unbalanced
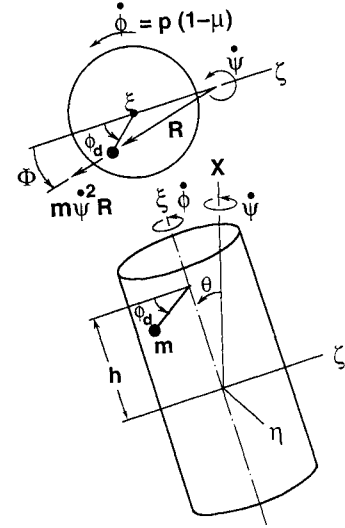

Fig. 2 Spacecraft precession damper.

rotor with a torque motor, for example, to produce the equivalent of a negative ϕ_d or Φ in Fig. 2 with a positive $\dot{\phi}$. Such devices have been developed.[7]

Vehicle Coning with Axial Thrust and Variable Mass

The variable mass accompanying thrust from a spin-stabilized rocket motor or PAM produces a destabilizing effect on coning due to a decrease in the lateral moment of inertia and a stabilizing effect from jet damping. Some authors include the variation of moment of inertia in their definition of jet damping. The net effect of the variable mass appears to be stabilizing for the solid rocket motor/payload configurations that have been investigated. The rocket thrust is a potential source of destabilizing yaw moment in the presence of a small mass imbalance relative to the precessing θ plane. These effects will be illustrated with somewhat simplistic models.

Consider the solid rocket motor shown in Fig. 3 in steady coning motion and assume, for simplicity, that the propellant burns in such a manner that the center of mass remains fixed. The total lateral rate is $\dot{\psi}\theta$, for small θ, and jet damping of this lateral rate produces an opposing yaw moment[24]

$$M_\zeta = \dot{M}\ell^2\dot{\psi}\theta \tag{23}$$

where $\dot{M}$ is the negative rate of change of vehicle mass from expended propellant and $-\dot{M}$ is the propellant mass flow rate. Similarly, it has been shown that a jet damping moment that opposes the rocket spin, due to spin momentum imparted to the ejected propellant gas, is of the form[25]

$$M_\xi = \dot{M}R^2 Fp \tag{24}$$

where R is some maximum radius of the mass of ejected gas, assumed to be in the form of a disk, and F is a function of the radial variation of the rotational velocity imparted to the gas. If we include variable moments of inertia in the angular momentum vector, Eq. (8), and substitute in the moment equations, Eq. (2), with the jet damping moments, Eqs. (23) and (24), we obtain

$$\dot{p} + \left(-\frac{\dot{M}R^2 F}{I_x} + \frac{\dot{I}_x}{I_x}\right)p = 0 \tag{25}$$

$$\dot{\psi} = \mu p \tag{26}$$

$$\dot{\theta} + \left(-\frac{\dot{M}\ell^2}{I} + \frac{\dot{I}}{I}\right)\theta = 0 \tag{27}$$

where we have assumed for quasi-steady coning motion that $\dot{\theta} \approx \ddot{\theta} \approx 0$ and $\dot{\psi} \approx$ const in the pitch equation. Because $\dot{I}_x/I_x$, $\dot{I}/I$, and $\dot{M}$ are negative, the variable mass effect on moment of inertia is destabilizing, whereas jet damping is stabilizing. If we make the
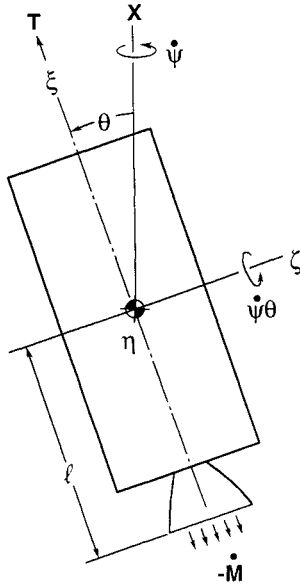
Fig. 3 Precessing rocket motor.

further assumption that the radius of gyration k in yaw remains constant, where $I = Mk^2$ and M is the vehicle mass at any instant, then the yaw equation, Eq. (27), can be written

$$\ddot{\theta} - \left(\frac{\ell^2}{k^2} - 1\right)\frac{\dot{M}}{M}\theta = 0 \tag{28}$$

and integrated to give

$$\theta = \theta_0\left(\frac{M}{M_0}\right)^{\left(\frac{\ell^2}{k^2}-1\right)} \tag{29}$$

The distance ℓ from the vehicle center of mass to the nozzle exit plane where the jet-damping force acts is, in general, larger than the yaw radius of gyration k, so that the net effect of the variable mass is stabilizing. Thomson and Reiter[26] analyzed variable mass effects on the coning motion of a solid rocket propelled spacecraft in which the vehicle center of mass displaced axially as the propellant burned. They found the net effects of variable mass to be stabilizing, consistent with flight data. Other complex flowfield analyses of variable mass effects on the PAM series of spin-stabilized vehicles[27,28] also showed the net effects of variable mass to be stabilizing, which fails to explain an observed coning instability exhibited by these vehicles toward the end of the motor burn. The jet damping moment, as defined in Refs. 27 and 28, includes the effect of variable yaw moment of inertia. It is noted in Ref. 28 that their numerical prediction of jet-damping moment is only 40–80% of the commonly used jet-damping moment obtained from one-dimensional flow theory, i.e., Eq. (23). It would appear from the foregoing analysis that this reduction in jet-damping moment is the destabilizing contribution from $\dot{I}/I$. The term $(\ell^2/k^2 - 1)$ compared with ℓ^2/k^2 is a measure of the reduction in jet damping due to the variable inertia.

Equation (25) is quite similar to Eq. (27) in that $\dot{I}_x/I_x$ has a destabilizing effect on the roll rate whereas the jet-damping term is, in general, stabilizing. If we take the maximum value R of the ejected propellant gases to be the nozzle exit radius and assume the rotational velocity varies linearly with radius, like a rigid body (per Ref. 25), then $F = 1/2$ and the jet-damping term is smaller in magnitude than $\dot{I}_x/I_x$ for typical PAM configurations. Even if the gas rotational velocity due to the rocket spin is constant with radius and equal to its maximum value at the nozzle exit radius, $F = 2/3$ and the destabilizing effect of $\dot{I}_x/I_x$ still exceeds the jet-damping such that the spin rate will increase. All of the PAM flight vehicles exhibited a small increase in spin rate during the coning divergence.

A possible explanation for the PAM instability is the yaw moment produced by the axial thrust acceleration acting on a small mass of liquified slag that accumulates in the aft end of the motor

as a byproduct of the propellant combustion. The mass would have to rotate or oscillate relative to the motor case such to maintain a position out of the $\zeta\xi$ or θ plane described by $0 < \phi_d < 180$ deg in Fig. 2 so that the thrust acceleration along ξ acting on the mass produces a positive yaw moment M_ζ. If the motion were such that the mass occupied the position $180 < \phi_d < 360$ deg, a negative yaw moment would be produced that would damp the coning motion. Mingori and Yam[15] considered a mass restrained by a radial spring oscillating in a plane perpendicular to ξ and located a distance h fore or aft of the center of mass, similar to that shown in Fig. 2 but with a spring restraining the mass. They came to the not surprising conclusion that the mass must lie out of the plane containing the transverse angular velocity vector (the $\xi\zeta$ plane of Fig. 3 in which $\dot{\psi}\theta$ is the transverse angular velocity about the ζ axis), such to produce a positive yaw moment. There is no satisfactory physical explanation for the spring-mass system parameters and the frequency required for instability, other than a loose analogy with fluid sloshing. More recent analyses with spherical pendulum models for the slag mass also required physically unrealizable parameters to match the observed PAM motions.[16,17] By comparison with the passive rotor or annular damper of Fig. 2, a small mass in the aft end of the motor subjected to centrifugal force from precession and a small viscous drag force would be driven out of the $\xi\zeta$ plane such to cause a negative yaw moment due to thrust that would damp the precession for a prolate vehicle ($\mu < 1$). Nevertheless, the amount of mass imbalance required to cause instability, if it is oriented properly, is so small that it merits further examination. We will illustrate this by assuming a buildup of slag in an appropriate orientation to produce a positive yaw moment due to thrust and estimate the amount of mass required, for typical PAM system parameters. We do not attempt to justify the assumed mass motion, which remains somewhat an anomaly.

Referring to Fig. 3, assume a linear buildup of mass $m = \dot{m}t$ in the aft end of the motor at $\eta = r$ in the precessing $\xi\eta\zeta$ coordinate system. The axial acceleration along ξ due to thrust will produce the positive yaw moment

$$M_\zeta = (Tmr/M) \tag{30}$$

which, when included with variable inertia and jet damping in the yaw equation, gives

$$\ddot{\theta} - \left(\frac{\ell^2}{k^2} - 1\right)\frac{\dot{M}}{M}\theta = \frac{T\dot{m}tr}{\mu pk^2M^2} \tag{31}$$

with the simplifying assumptions of fixed center of mass and constant yaw radius of gyration. If we assume that $\dot{M}$ is a negative constant such that the vehicle mass M decreases linearly from its initial value at ignition to its final value at burnout, we can integrate Eq. (31) for the coning growth caused by the mass m. The results are shown in Fig. 4 for only 5 lb (2.27 kg) of mass buildup in the 85-s burn time, with the vehicle properties of Table 1 and with $\ell^2/k^2 - 1$ selected to give 40–80% of jet damping corresponding to the results of Ref. 28. The assumed slag buildup is only 0.1% of the burned propellant mass. Although there appears to be no satisfactory physical explanation for the mass motion prescribed to obtain these results, the example illustrates the surprisingly small amount of mass required to cause the coning divergence and the extreme sensitivity of the spinning vehicle motion to a yaw moment.

Table 1 Assumed PAM/spacecraft parameters

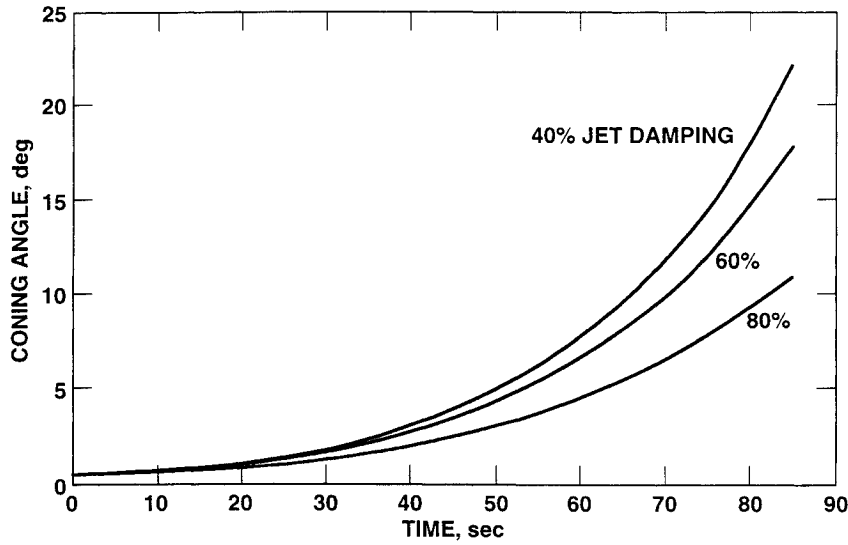| |
| --- |
| Initial weight, $M_0g = 7200$ lb (3266 kg) |
| Weight loss, $\dot{M}g = -52$ lb/s (-23.6 kg/s) |
| Yaw radius of gyration, $k = 3$ ft (0.914 m) |
| Inertia ratio, $\mu = 0.4$ |
| Roll rate, $p = 300$ deg/s |
| Thrust, $T = 13,000$ lb (57,827 N) |
| Slag buildup rate, $\dot{m}g = 5$ lb/85 s (0.0267 kg/s) |
| Slag radial position, $r = 1.5$ ft (0.457 m) |
| Initial coning angle, $\theta_0 = 0.5$ deg |

Fig. 4   Potential PAM coning divergence from 5 lb (2.27 kg) slag buildup.

Missile Equations of Motion

The dynamics of spinning, nominally axisymmetric missiles are commonly described in terms of body-fixed coordinates[29] or aeroballistic coordinates that pitch and yaw with the missile but do not roll.[1-4] Because the aerodynamic forces and moments are functions of the missile angles of attack and sideslip, which depend on the lateral translations of the missile relative to its forward velocity, a rigorous formulation of the missile equations must include the coupled translational and rotational equations of motion, Eqs. (1) and (2). We can obtain an approximate description of the missile motion in terms of the Euler angle moment equations, Eqs. (9–11), to show the similarity of spacecraft and missile yaw moment instabilities.

Consider an axisymmetric missile in quasisteady coning motion about the mean flight path, as shown in Fig. 5, and assume that the missile is statically stable, i.e., there is a lift force $L = L_\theta \theta$ proportional to θ that acts aft of the center of mass a distance x_s (the static margin) such to produce a restoring moment $L x_s$ that tends to reduce θ. The missile center of mass translates around the mean flight path such that the lift force, ignoring gyroscopic spin effects, balances the centrifugal force due to precession according to

$$L = m\dot{\psi}^2 r \qquad (32)$$

where

$$r = \ell\theta \qquad (33)$$

If we consider the missile rotational motion in the precessing Euler angle coordinate frame, Fig. 1, and let the missile axis lie along ξ, then the restoring moment $L x_s$ is $-M_\eta$, which is defined in terms of the natural pitch frequency $\omega = (L_\theta x_s/I)^{\frac{1}{2}}$ according to

$$\frac{M_\eta}{I} = -\frac{L x_s}{I} = -\omega^2 \theta \qquad (34)$$

If we substitute Eq. (34) into Eq. (10) and assume $\ddot{\theta} \approx 0$, we can write the pitch equation

$$(\omega^2 + \mu p\dot{\psi} - \dot{\psi}^2)\theta = 0 \qquad (35)$$

which, for nonzero θ, gives the two precession frequencies

$$\dot{\psi}_{+,-} = p_r \pm \Omega \qquad (36)$$

For slender missiles, $\mu \ll 1$, and roll rates of the order of or less than the pitch frequency, the precession frequencies are approximately
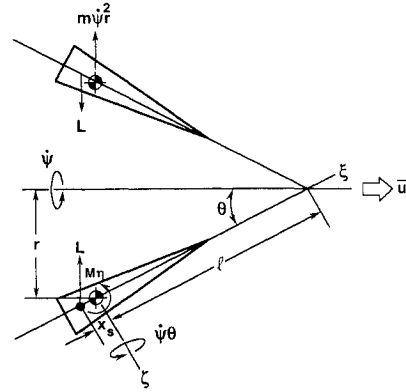
$$\dot{\psi}_{+,-} = \pm\omega \qquad (37)$$

Fig. 5   Coning, statically stable missile.

The length l from the missile center of mass to the center of precession can be obtained from Eqs. (32) and (33) with the result, Eq. (37), for the precession frequencies, and is found to be

$$\ell = I/mx_s = k^2/x_s \qquad (38)$$

Note that the coning angle θ in Fig. 5 is not the missile total angle of attack. Because the missile has a lateral velocity $v = \dot{\psi}r$, as shown in Fig. 6, looking forward along the mean flight path, there is a component of angle of attack normal to θ of magnitude v/u. This angle attack component is proportional to θ and is found to be

$$\frac{v}{u} = \frac{\omega\ell\theta}{u} \qquad (39)$$

which is quite small, in general, relative to θ. The total angle of attack Θ is then

$$\Theta = \left[\theta^2 + \left(\frac{v}{u}\right)^2\right]^{1/2} \approx \theta\left[1 + \frac{1}{2}\left(\frac{\omega\ell}{u}\right)^2\right] \qquad (40)$$

Although the lateral velocity contribution to total angle of attack is generally quite small, it has an appreciable effect in damping the coning motion, i.e., the normal force or lift force proportional to this angle-of-attack component always opposes the coning motion irrespective of whether $\dot{\psi}$ is positive or negative (clockwise or counterclockwise). Note also, from Fig. 5, that a coning missile has a component of lateral rate $\dot{\psi}\theta$ about the yaw axis ζ. Aerodynamic forces that oppose this lateral rate or tumbling motion also damp the coning motion irrespective of its direction and add to the lateral force damping.
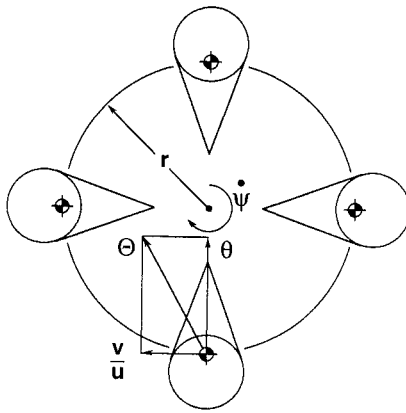
Fig. 6   Precessing missile viewed along flight path.

Yaw Moment Undamping

A rigorous derivation of the linearized, small-angle, constant roll rate equations of motion in terms of the total angle of attack Θ and including aerodynamic damping and a Magnus moment (to be described later) gives for the yaw moment equation[30–32]

$$(2\dot{\psi} - \mu p)\dot{\Theta} + (\nu\dot{\psi} - \nu_m p)\Theta = 0 \tag{41}$$

where $\dot{\psi}$ has two modes, as defined in Eq. (36) or (37), and ν and ν_m are defined in terms of aerodynamic coefficients by

$$\nu = C_{m_q}^* + C_{m_{\dot{\alpha}}}^* + C_{L_\alpha}^* \tag{42}$$

$$\nu_m = \mu C_{L_\alpha}^* + C_{n_{p\alpha}}^* \tag{43}$$

Equation (41) is of the form

$$\dot{\Theta} + \lambda_{+,-}\Theta = 0 \tag{44}$$

where $\lambda_{+,-}$, with $\dot{\psi}$ defined by Eq. (36), is

$$\lambda_{+,-} = \frac{1}{2}\left(\nu \pm \frac{\sigma}{\Omega}\right) \tag{45}$$

$$\sigma = \nu p_r - \nu_m p \tag{46}$$

and has the solution

$$\Theta = \Theta_0 \exp(\lambda_{+,-}t) \tag{47}$$

The motion described by Eqs. (47) and (36), expressed in terms of the complex angle of attack $\tilde{\xi} = \tilde{\beta} + i\tilde{\alpha}$ in the aeroballistic coordinate system, is the damped epicyclic motion[30–32]

$$\tilde{\xi} = K_+ \exp(\lambda_+ + i\dot{\psi}_+)t + K_- \exp(\lambda_- + i\dot{\psi}_-)t \tag{48}$$

where K_+ and K_- are determined from the initial conditions. The parameter ν in $\lambda_{+,-}$, which includes the lateral force plus lateral rate damping coefficients, is normally positive and damps both coning motions. The parameter σ, which includes the Magnus moment coefficient $C_{n_{p\alpha}}^*$, has a damping effect on one coning motion and an undamping effect on the other. If the roll rate and Magnus coefficient are large enough that σ/Ω exceeds ν in magnitude, the exponent becomes positive for one of the coning motions and the coning angle can grow to large values. The Magnus instability is a classical case of yaw moment undamping as illustrated in Fig. 7. The crossflow velocity due to angle of attack adds to the boundary-layer velocity due to roll on one side of the vehicle and subtracts from this velocity on the other side to produce a net Magnus force or side force normal to the θ plane. If this force is produced aft of the center of mass, for example, then the moment produced about the center of mass is the positive yaw moment M_ζ that undamps the positive coning motion and damps the negative coning motion.

A striking example of a Magnus-type instability occurred with a finned re-entry vehicle.[33] The fins were canted to produce a positive
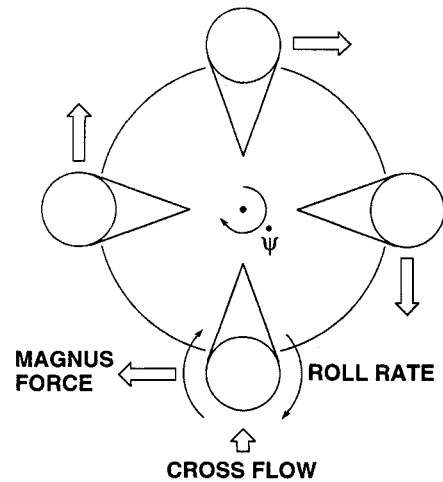

Fig. 7   Magnus instability.

(clockwise) roll torque. Because the windward fin is more effective than the leeward fin, with the vehicle at angle of attack, a net side force, or yaw force, is produced that is approximately proportional to the angle of attack. Although the mechanism for side force generation is appreciably different from that of the classical Magnus force and is independent of roll rate to the first order, the net effect is a yaw moment undamping that can grow catastrophically, hence, the designation "Magnus-type" instability. There are many other sources of side force and Magnus-type instabilities with spinning missiles, including the effects of re-entry vehicle ablation time lag,[34] asymmetric boundary-layer transition,[35] and vortex shedding at angle of attack.[36,37] A particularly illustrative example of yaw-moment undamping is roll resonance lock-in from mass and configurational asymmetries, which is described in the next section.

The missile dynamic stability is determined by the sign of the exponents in Eqs. (47) and (48). For the missile to remain dynamically stable, the exponent must remain negative for both precession modes. An extensive review of symmetric missile dynamic instabilities is contained in a paper by Murphy,[38] who considers linear and nonlinear Magnus moments, nonlinear static and damping moments, configurational asymmetries, effects of moving internal parts, roll-induced side moments, unequal pitch and yaw frequencies, and other aerodynamic phenomena. In most cases, dynamic instability can be attributed to a yaw moment or to side forces such as the Magnus force of Fig. 7 that have a component normal to the θ plane that acts fore or aft of the missile center of mass to produce a yaw moment.

Roll Resonance Lock-In

Another classical example of a yaw moment instability is roll resonance lock-in caused from mass and configurational asymmetries.[5,39–44] Consider a nominally axisymmetric missile with small body-fixed asymmetries consisting of a radial offset y of the center of mass from the aerodynamic axis of symmetry and an orthogonal trim force asymmetry τ that produces a zero roll rate trim angle of attack Θ_T, as shown in Fig. 8a. A quasisteady solution of the moment equations of motion for the total angle of attack Θ yields the result[32]

$$\frac{\Theta}{\Theta_T} = [(1 - \lambda^2)^2 + (2\zeta\lambda)^2]^{\frac{-1}{2}} \tag{49}$$

$$\phi = \tan^{-1}\left(\frac{2\zeta\lambda}{1 - \lambda^2}\right) \tag{50}$$

where $\lambda = p/p_{crit}$ is the ratio of the roll rate to the critical roll rate, $p_{crit} = \omega/(1 - \mu)^{\frac{1}{2}}$, and $2\zeta = (\nu - \mu C_{L_\alpha}^*)/\omega(1 - \mu)^{\frac{1}{2}}$. Note from Eq. (50) and Fig. 8b that for subcritical roll rates ($\lambda < 1$) ϕ is positive and the positive roll torque produced by the lift force acting on the moment arm $y \cos\phi$ increases the roll rate toward resonance, $\lambda = 1$. For any positive value of ϕ the trim component $\tau \sin\phi$ is a
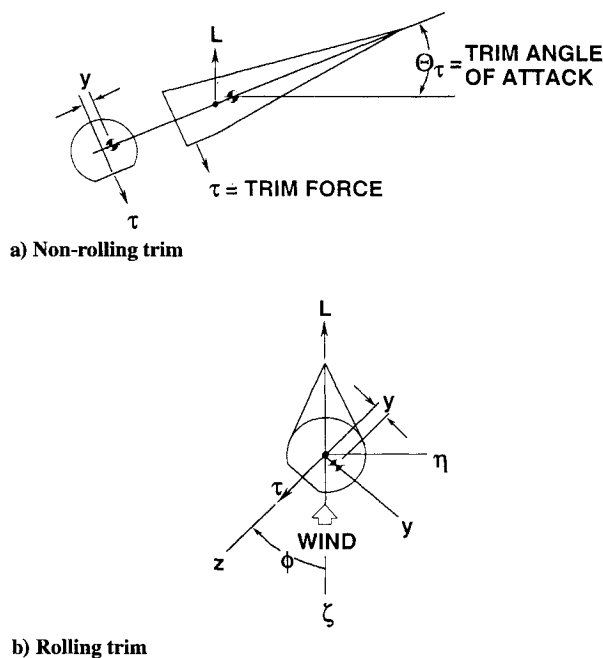
a) Non-rolling trim

b) Rolling trim

Fig. 8 Orthogonal mass and configurational asymmetries.

yaw force that produces the yaw moment $M_\zeta / I = \omega^2 \Theta_T \sin \phi$ and undamps the angle of attack. As the roll rate approaches critical, $\lambda \to 1$, $\phi \to 90$ deg, the trim angle of attack is amplified according to Eq. (49), which rapidly increases the lift force and the roll torque and drives the missile into a "resonance lock-in" condition. Similarly, for initially supercritical roll rates, $\lambda > 1$, ϕ is negative, which produces a negative roll torque that drives the roll rate down into resonance. Thus, the roll rate is driven into the stable equilibrium condition of steady roll resonance, $\lambda = 1$, in which the trim angle of attack Θ_T is amplified by the resonance amplification factor $1/2\zeta$ from Eq. (49). The phenomenon is termed roll resonance because the resonance amplification of the trim angle of attack, expressed by Eqs. (49) and (50), is analogous to the resonance amplification of a damped, single-degree-of-freedom oscillator. At steady resonance ($\phi = 90$ deg) the body-fixed trim angle of attack produces a pure yaw moment, which effectively undamps the rolling trim angle of attack coning motion. Other examples of roll-resonance-induced yaw moment instabilities are described in the literature.[45-49]

Concluding Remarks

The foregoing derivations of the coning motions of spinning, axisymmetric bodies, with selected examples of classical missile and spacecraft coning instabilities, illustrate the extreme sensitivity of missile and spacecraft motion to yaw moment disturbances. The analyses were performed in the classical Euler angle coordinate system, which elucidates the description of the yaw moment and facilitates the analyses. The yaw moment is simply the net moment acting about one of the coordinate axes in the precessing Euler angle system. It has been shown that the general motion of a spinning axisymmetric body consists of a precession about the resultant angular momentum vector plus a spin of the body about its axis of symmetry relative to the precessing plane that defines the coning angle. The rate and direction of this spin depends on the ratio of the roll to transverse mass moment of inertia, which can have a strong influence on yaw moments generated by small missile and spacecraft components free to move relative to the spinning body. It has been shown that very small asymmetries, consisting of either mass or configurational asymmetries or combinations thereof, can produce small yaw moments sufficient to destabilize the motion, sometimes leading to catastrophic failures. It is hoped that the viewpoint expressed in this paper has provided the reader a bit more insight into the mechanics of yaw moment undamping and can, perhaps, help the missile or spacecraft designer to avoid the occurrence of such instabilities in future designs.

References

[1]Fowler, R. H., Gallop, E. G., Lock, C. N. H., and Richmond, H. W., "The Aerodynamics of a Spinning Shell," *Philosophical Transactions of the Royal Society of London, Series A: Mathematical and Physical Sciences*, Vol. 221, 1920, pp. 295–387.

[2]McShane, E. G., Kelley, J. L., and Reno, F. V., *Exterior Ballistics*, Univ. of Denver Press, Denver, CO, 1953.

[3]Nicolaides, J. D., "On the Free Flight Motion of Missiles Having Slight Configurational Asymmetries," U.S. Army Ballistic Research Lab., Rept. 858, June 1953.

[4]Murphy, C. H., "Free-Flight Motion of Symmetric Missiles," U.S. Army Ballistic Research Lab., Rept. 1216, July 1963.

[5]Nicolaides, J. D., "Two Nonlinear Problems in the Flight Dynamics of Modern Ballistic Missiles," Inst. of the Aeronautical Sciences, Rep. 59–17, Jan. 1959.

[6]Thomson, W. T., *Introduction to Space Dynamics*, Wiley, New York, 1961, pp. 212–214.

[7]Hopper, F. W., "Active Precession Control for Spin Stabilized Space Vehicles," AIAA Paper 71-952, 1971.

[8]Carrier, G. F., and Miles, J. W., "On the Annular Damper for a Freely Precessing Gyroscope," *Journal of Applied Mechanics*, Vol. 27, No. 2, 1960, pp. 237–240.

[9]Stewartson, K., "On the Stability of a Spinning Top Containing Liquid," *Journal of Fluid Mechanics*, Vol. 5, Pt. 4, 1959, pp. 577–592.

[10]Soper, W. G., "Projectile Instability Produced by Internal Friction," *AIAA Journal*, Vol. 16, No. 1, 1978, pp. 8–11.

[11]Murphy, C. H., "Influence of Moving Internal Parts on Angular Motion of Spinning Projectiles," *Journal of Guidance, Control, and Dynamics*, Vol. 1, No. 2, 1978, pp. 117–122.

[12]Miller, M. C., "Flight Instabilities of Spinning Projectiles Having Non-rigid Payloads," *Journal of Guidance, Control, and Dynamics*, Vol. 5, No. 2, 1982, pp. 151–157.

[13]Meyer, R. X., "Convective Instability in Solid Propellant Rocket Motors," *Astrodynamics 1983*, Vol. 54, I and II, Advances in the Astronautical Sciences, 1983, pp. 657–669.

[14]Flandro, G. A., "Generation of Vehicle Wobbling by the Unsteady Flow Field in a Spinning Solid Propellant Rocket Motor," *Proceedings of the 20th JANNAF Combustion Meeting*, Vol. 1, 1983, pp. 181–192.

[15]Mingori, D. L., and Yam, T., "Nutational Stability of a Spinning Space-craft with Internal Mass Motion and Axial Thrust," AIAA Paper 86-2271, 1986.

[16]Cochran, J. E., Jr., and Kang, J. Y., "Nonlinear Stability Analysis of the Attitude Motion of a Spin-Stabilized Upper Stage," AAS/AISS Spaceflight Mechanics Meeting, AAS Paper 91-109, Houston, TX, Feb. 1991.

[17]Or, A. C., "Rotor-Pendulum Model for the Perigee Assist Module Nutation Anomaly," *Journal of Guidance, Control, and Dynamics*, Vol. 15, No. 2, 1992, pp. 297–303.

[18]Crout, P. D., "Theoretical Investigation of the Dynamic Behavior of the Mercury Damper," U.S. Naval Ordnance Test Station, NAVWEPS Rept. 8611, NOTS TP3635, China Lake, CA, Nov. 1964.

[19]Cartwright, W. F., Massingill, E. C., and Trueblood, R. D., "Circular Constraint Nutation Damper," *AIAA Journal*, Vol. 1, No. 6, 1963, pp. 1375–1380.

[20]Alfriend, K. T., "Partially Filled Viscous Ring Nutation Damper," *Journal of Spacecraft and Rockets*, Vol. 11, No. 7, 1974, pp. 456–462.

[21]Bhuta, P. G., and Koval, L. R., "A Viscous Ring Damper for a Freely Precessing Satellite," *International Journal of Mechanical Sciences*, Vol. 8, 1966, pp. 383–395.

[22]Miles, J. W., "On the Annular Damper for a Freely Precessing Gyroscope—II," *Journal of Applied Mechanics*, Vol. 30, No. 2, 1963, pp. 189–192.

[23]Chang, C. O., Chou, C. S., and Wang, S. Z., "Design of a Viscous Ring Nutation Damper for a Freely Precessing Body," *Journal of Guidance, Control, and Dynamics*, Vol. 14, No. 6, 1991, pp. 1136–1144.

[24]Thomson, W. T., *Introduction to Space Dynamics*, Wiley, New York, 1961, pp. 221–223.

[25]Murphy, C. H., "Spin Jet Damping of Rocket-Assisted Projectiles," *Journal of Guidance, Control, and Dynamics*, Vol. 4, No. 3, 1981, pp. 350, 351.

[26]Thomson, W. T., and Reiter, G. S., "Jet Damping of a Solid Rocket: Theory and Flight Results," *AIAA Journal*, Vol. 3, No. 3, 1965, pp. 413–417.

[27]Murdock, J. W., and Meyer, R. X., "The Stability of a Precessing Vehicle with Outflow," The Aerospace Corp., Rept. TR-0089(4464-06)-1, El Segundo, CA, April 1991.

[28]Misterek, D., Murdock, J., and Koshigoe, S., "Gas Dynamic Flow in a Spinning, Coning Solid Rocket Motor," AIAA Paper 91-1671, June 1991.

[29]Nelson, R. L., "The Motions of Rolling Symmetrical Vehicles Referred to a Body Axis System," NACA TN 3737, Nov. 1956.

[30]Murphy, C. H., "Comment on Angle-of-Attack Convergence and Windward Meridian Rotation Rate of Rolling Re-Entry Vehicles," *AIAA Journal*, Vol. 8, No. 7, 1970, pp. 1372–1374.

[31]Platus, D. H., "Reply by Author to C. H. Murphy," *AIAA Journal*, Vol. 8, No. 7, 1970, pp. 1374, 1375.

[32]Platus, D. H., "Ballistic Re-Entry Vehicle Flight Dynamics," *Journal of Guidance, Control, and Dynamics*, Vol. 5, No. 1, 1982, pp. 4–16.

[33]Platus, D. H., "Dynamic Instability of Finned Missiles Caused by Unbalanced Fin Forces," *AIAA Journal*, Vol. 9, No. 3, 1971, pp. 378–381.

[34]Waterfall, A. P., "Effect of Ablation on the Dynamics of Spinning Re-Entry Vehicles," *Journal of Spacecraft and Rockets*, Vol. 6, No. 9, 1969, pp. 1038–1044.

[35]Crusciel, G. T., "RV Lateral Force Characteristics During Boundary Layer Transition," *Proceedings of the AIAA Atmospheric Flight Mechanics Conference*, AIAA, New York, 1977, pp. 266–274 (AIAA Paper 77-1151).

[36]Tobak, M., Schiff, L. B., and Peterson, V. L., "Aerodynamics of Bodies of Revolution in Coning Motion," *AIAA Journal*, Vol. 7, No. 1, 1969, pp. 95–99.

[37]Schiff, L. B., and Tobak, M., "Results from a New Wind-Tunnel Apparatus for Studying Coning and Spinning motions of Bodies of Revolution," *AIAA Journal*, Vol. 8, No. 11, 1970, pp. 1953–1957.

[38]Murphy, C. H., "Symmetric Missile Dynamic Instabilities A Survey," *Journal of Guidance and Control*, Vol. 4, No. 5, 1981, pp. 464–471.

[39]Glover, L., "Effects on Roll Rate of Mass and Aerodynamic Asymmetries for Ballistic Re-Entry Bodies," *Journal of Spacecraft and Rockets*, Vol. 2, No. 2, 1965, pp. 220–225.

[40]Pettus, J. J., "Persistent Re-Entry Vehicle Roll Resonance," AIAA Paper 66-49, Jan. 1966.

[41]Platus, D. H., "A Note on Re-Entry Vehicle Roll Resonance," *AIAA Journal*, Vol. 5, No. 7, 1967, pp. 1348–1350.

[42]Price, D. A., Jr., "Sources, Mechanisms, and Control of Roll Resonance Phenomena for Sounding Rockets," *Journal of Spacecraft and Rockets*, Vol. 4, No. 11, 1967, pp. 1516–1525.

[43]Vaughn, H. R., "Boundary Conditions for Persistent Roll Resonance on Re-Entry Vehicles," *AIAA Journal*, Vol. 6, No. 6, 1968, pp. 1030–1035.

[44]Price, D. A., Jr., and Ericcson, L. E., "A New Treatment of Roll-Pitch Coupling for Ballistic Re-Entry Vehicles," *AIAA Journal*, Vol. 8, No. 9, 1970, pp. 1608–1615.

[45]Clare, T. A., "Resonance Instability for Finned Configurations Having Nonlinear Aerodynamic Properties," *Journal of Spacecraft and Rockets*, Vol. 8, No. 3, 1970, pp. 278–283.

[46]Pepitone, T. R., and Jacobson, I. D., "Resonant Behavior of a Symmetric Missile Having Roll Orientation-Dependent Aerodynamics," *Journal of Guidance and Control*, Vol. 1, No. 5, 1978, pp. 335–339.

[47]Hodapp, A. E., Jr., "Effects of Unsymmetrical Stability Derivative Characteristics on Re-Entry Vehicle Trim Angle Behavior," *Journal of Spacecraft and Rockets*, Vol. 11, No. 5, 1974, pp. 300–307.

[48]Hodapp, A. E., Jr., "Effects of Unsymmetrical Stability Derivative Characteristics on Re-Entry Vehicle Transient Angular Motion," *Journal of Spacecraft and Rockets*, Vol. 13, No. 2, 1976, pp. 82–90.

[49]Murphy, C. H., "Some Special Cases of Spin-Yaw Lock-in," *Journal of Guidance, Control, and Dynamics*, Vol. 12, No. 6, 1989, pp. 771–776.